Structure Stability and Growth Strategies of the $(MgO)_n$ (n=1-13) Clusters

Zhen ZHAO[1,a], Di WANG[2,b], Qi WANG[2,c,*] and Zhi LI[2,d]

[1]School of Chemistry and Life Science, Anshan Normal University, Anshan 114007, PR China

[2]School of Materials and Metallurgy, University of Science and Technology Liaoning, Anshan 114051, PR China

[a]email:zhaozhenlunwen@yeah.net, [b]email:wangdinow@163.com, [c]email:wangqi8822@sina.com, [d]email:lizhi81723700@163.com

*Corresponding author:wangqi8822@sina.com

Keywords: MgO cluster, Stability, Growth strategies, Density functional theory

Abstract. The thermal decomposition process of magnesite significantly affects the catalytic activity of MgO. The structure, stability and growth strategies of the $(MgO)_n$ (n = 1-13) clusters were investigated by density functional theory. From reaction energy it can be seen that the contributions of the small clusters to grow are larger at lower temperature. By analyzing the differences in Gibbs free energy between MgO crystal and $(MgO)_n$ clusters, it can be seen that at the initial decomposition temperature of magnesite (about 700K), the $(MgO)_n$ clusters with linear or distorted cubic structures become more stable than the hexagon ring structures, even the hybrid structures are more stable than the cage structures.

Introduction

The study of clusters allows a better understanding of the evolution of the main physical properties of systems [1]. Characteristics of cluster growth are major important to develop nanotechnology and nano-catalysis [2]. Magnesite is present at the Earth's surface to deep mantle [3]. Accurate control of the thermal decomposition of magnesite in industry is necessary to achieve a high reactivity [4]. Fu et al. [5] observed the grain size of MgO during the thermal decomposition of magnesite by the X-ray line broadening technique. These experimental results reflect the information after product nucleation, but it is difficult to analyze the nucleation mechanism. A detailed understanding of the growth of $(MgO)_n$ clusters will lead to an improved understanding of epitaxial growth of MgO surfaces [6]. The research on the $(MgO)_n$ clusters has typical significance to cage-like metal oxide clusters.

In this work, a first-principles method is used to calculate the stability of $(MgO)_n$ (n=1-13) clusters. How the growth strategy changes with the temperature for the $(MgO)_n$ clusters will be discussed.

Computational Details

The stable structures of $(MgO)_n$ clusters (Fig.1) were adopted from Ref. [1-2,6-12]. Our calculations were performed using the spin polarized density functional theory (DFT) implemented in the DMol^3 package [13,14] within the generalized gradient approximation (GGA) using the BLYP hybrid exchange functional [15,16]. The double numerical polarization (DNP) basis set was adopted [13], and effective core potentials were used. We observed the following convergence thresholds for geometry optimization: total energy convergence tolerance 1.0×10^{-5} Ha steps, 2×10^{-3} Ha/Å for maximum force and 5×10^{-3} Å for maximum displacement. The energy gradient and atomic displacements converged to within 1×10^{-5} Hartree/Bohr and 5×10^{-3} Å, respectively. In self-consistent calculation, charge density tolerance 1.0×10^{-6} e/Å^3, smearing were set to 5.0×10^{-5} Ha.

For the lowest-energy structures of $(MgO)_n$ (n=1-13), only $(MgO)_m+(MgO)_{n-m}\rightarrow(MgO)_n$ aggregation model was considered. The reaction energy ΔE was defined as

$$\Delta E = [(E_m + E_{n-m}) - E_n]/n \tag{1}$$

The vibration spectrum can also be calculated to get the thermodynamic properties. The difference in Gibbs free energy between MgO crystal and $(MgO)_n$ clusters is

$$\Delta G = G_{MgO(crystal)} - \frac{1}{n} G_{(MgO)_n} \tag{2}$$

Results and Discussions

Structures of $(MgO)_n$ Clusters

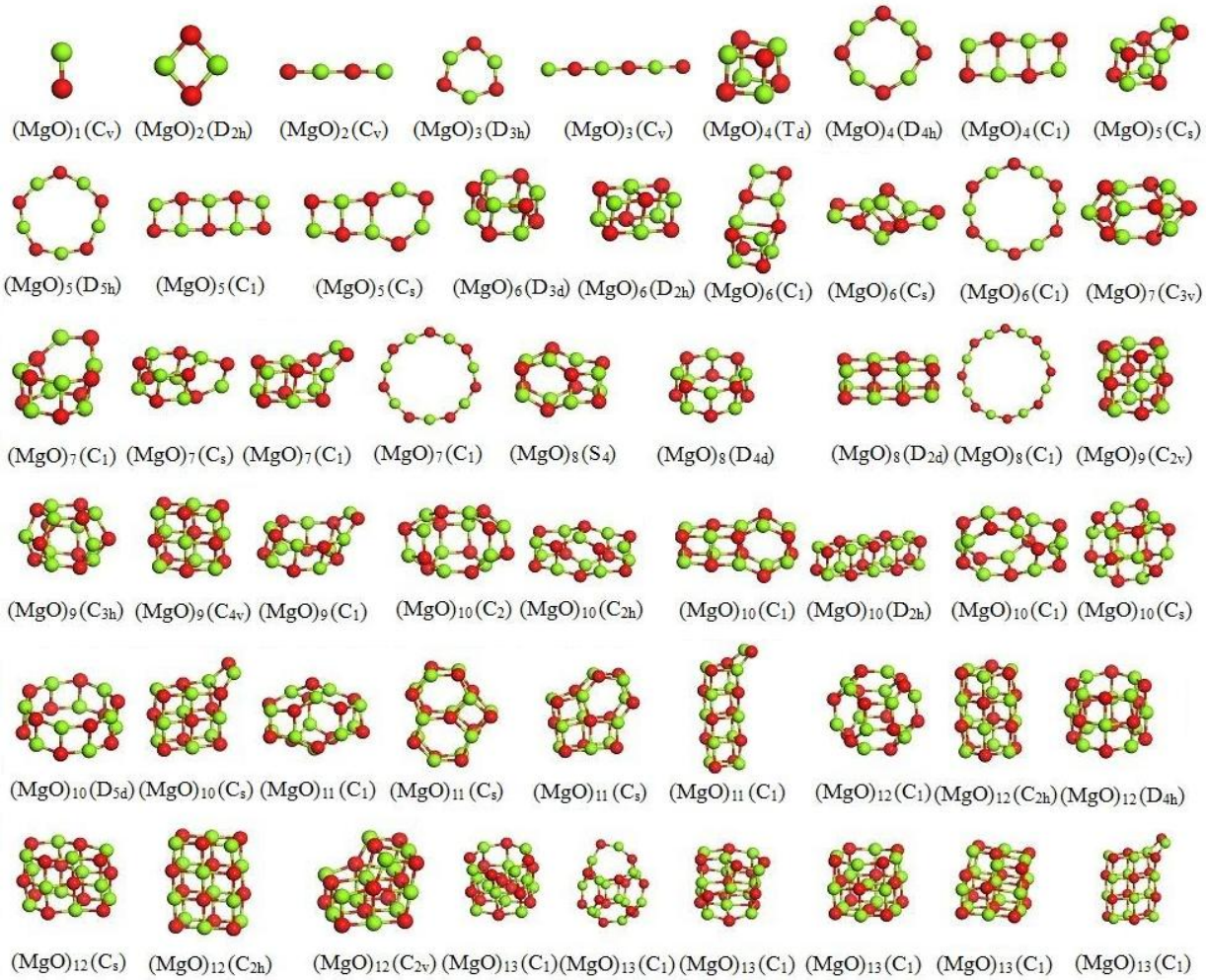

Fig. 1. The lowest-energy configurations and low-lying isomers of $(MgO)_n$ (n = 1-13) clusters. (Lawngreen ball: Mg atom, and red ball: O atom).

The optimized structures of low-lying isomers of $(MgO)_n$ (n=1-13) are shown in Fig.1. To verify the accuracy of calculation, the bond length (r= 1.790 Å) of the linear structure (C_v) MgO is compared with the other calculated data (r= 1.76Å[1], 1.749Å[1], 1.739Å[17], 1.733Å[17], 1.751Å[17], 1.739Å[18],1.75Å[12]). The bond length is 1.894Å (1.88Å[12]) in the most favorable structure of $(MgO)_2$ which is a rhombus structure (D_{2h}). The other linear structure (C_v) is 1.301 eV higher in energy than the quadrilateral ring (D_{2h}). The lowest-energy structure of $(MgO)_3$ is the hexagonal ring isomer (D_{3h}). The bond angles at oxygen ions are smaller than at magnesium ions,

but the Mg-O bond lengths remain the same within this planar structure [12]. The other (C_v) structure is 2.704 eV higher in energy than the hexagonal ring (D_{3h}). From n = 4 on, the three-dimensional structures are favored. Our result from n=4 is different from those in Ref. [12] in which the two low-lying isomers were found not to be C_1 and D_{4h} in sequence. The hybrid structure C_s for $(MgO)_5$ has not been mentioned in Ref.[12].

Stability of $(MgO)_n$ Clusters

This calculated binding energies are slightly lower than that by LDA theory[1], but they are slightly larger than that by BL3YP and 6-311G(d) theory[2]. The calculated $\Delta E_{b,n}$ and $\Delta E^2_{b,n}$ for the considered $(MgO)_n$ (n=1-13) clusters are plotted in Fig. 2. It found that the maximum of $\Delta E_{b,n}$ for $(MgO)_n$ is n=6,12. It means that $(MgO)_6$ and $(MgO)_{12}$ cluster have a higher stability. The second-order differences $\Delta E^2_{b,n}$ for $(MgO)_n$ demonstrate that the Hexagonal ring D_{3d} $(MgO)_6$ and cage structure $(MgO)_{12}$ are more stable. The small clusters also show a preference for the hexagonal tubes which are stacked by the $(MgO)_3$ hexagons, and they have been confirmed by infrared spectra for $(MgO)_{3n}$ (n = 2–5) [19] and the mass spectrum of MgO clusters [20]. The covalent interaction in small MgO clusters is responsible for the preferable stability of the hexagonal tubes over the rock-salt structures [21].

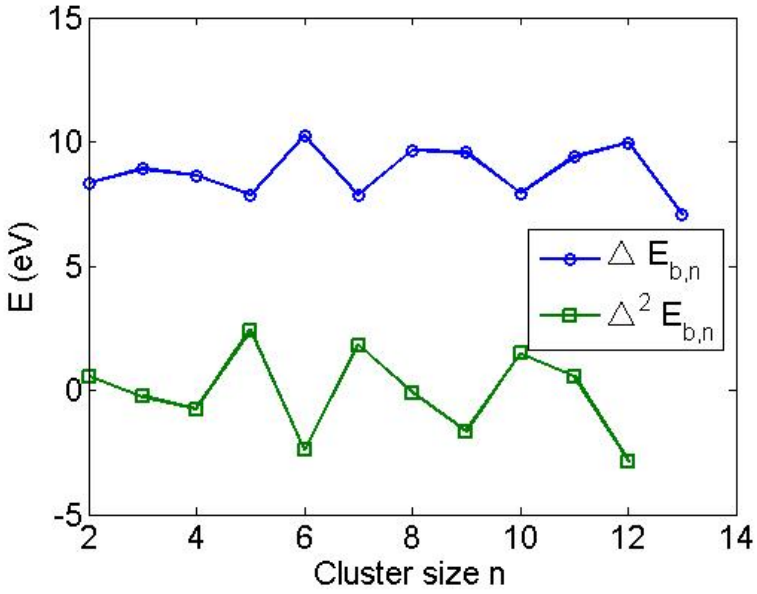

Fig. 2. Size dependence of the $\Delta E_{b,n}$ and ΔE^2_n for the $(MgO)_n$ (n = 1-13) clusters.

Growth Strategies of $(MgO)_n$ Clusters

To understand the growth strategies of the $(MgO)_n$ clusters at lower temperature, the reaction energies are listed in Table 1. For the same cluster size n, from the largest ΔE it can be seen the contributions of $(MgO)_1$, $(MgO)_1+(MgO)_1\rightarrow(MgO)_2$> $(MgO)_1+(MgO)_2\rightarrow(MgO)_3$ > $(MgO)_1+(MgO)_5\rightarrow(MgO)_6$. $(MgO)_2$, $(MgO)_1+(MgO)_2\rightarrow(MgO)_3$> $(MgO)_2+(MgO)_2\rightarrow(MgO)_4$>$(MgO)_2+(MgO)_3\rightarrow(MgO)_5$> $(MgO)_2+(MgO)_5\rightarrow(MgO)_7$. $(MgO)_3$, $(MgO)_2+(MgO)_3\rightarrow(MgO)_5$> $(MgO)_3+(MgO)_5\rightarrow(MgO)_8$; $(MgO)_4$, $(MgO)_4+(MgO)_5\rightarrow(MgO)_9$> $(MgO)_4+(MgO)_7\rightarrow(MgO)_{11}$... In a word, the contributions of the small clusters to grow at lower temperatures as follows:$(MgO)_1$>$(MgO)_2$>$(MgO)_3$>$(MgO)_4$>$(MgO)_5$>$(MgO)_7$>$(MgO)_8$>... It can also be seen that the reaction energy has the magic number character.

Table 1. The ΔE of $(MgO)_m+(MgO)_{n-m}\rightarrow(MgO)_n$ [eV/atom]

	m=1	m=2	m=3	m=4	m=5	m=6
n=2	1.3353					
n=3	0.9832					
n=4	0.7044	0.7741				
n=5	0.4865	0.5159				
n=6	0.6061	0.5664	0.5444			
n=7	0.3465	0.4845	0.4106			
n=8	0.4171	0.3865	0.4724	0.4242		
n=9	0.3652	0.4393	0.3811	0.4721		
n=10	0.2457	0.3074	0.3461	0.3069	0.4273	
n=11	0.2905	0.2710	0.3017	0.3490	0.3483	
n=12	0.2898	0.3335	0.2925	0.3316	0.4070	0.3061
n=13	0.1570	0.2191	0.2380	0.2103	0.2760	0.2530

To further understand the growth strategies of the $(MgO)_n$ clusters as the temperature increased, Table 2 lists the ΔG between MgO crystal and various structures for $(MgO)_n$ clusters with the sequence in Fig.1 as the initial thermal decomposition temperature of magnesite 700 K[22-25]. From Table 2 it can be seen that ΔG is less than zero as n>7, it means that $(MgO)_n$ (n>7) clusters begin to spontaneously grow at 700K. For $(MgO)_4$, stair-type fused rhombi (C_1) becomes easier to gather than octagonal rings structure D_{4h}. For $(MgO)_5$, fused rhombi structure C_1 and hybrid structure C_s become easier to assemble than ten-member ring structure D_{5h}. The lowest-energy structure of $(MgO)_6$ becomes the distorted cubic structure (D_{2h}) instead of the stacked double ring structure (D_{3d}). For $(MgO)_7$, hybrid structures based on distorted cubic structure are more stable than that based on hexagon ring structure. For $(MgO)_8$, the lowest-energy structure becomes distorted cubic D_{2d} isomer rather than the hybrid structure (S_4). For $(MgO)_9$, the stability of distorted cubic C_{4v} becomes higher than that of cage structure C_{3h}. For $(MgO)_{10}$, the calculated lowest-energy structure becomes distorted cubic D_{2h} other than cage structure (C_2), and even the hybrid structures based on stacked distorted cubic are more stable than the other isomers. For $(MgO)_{11}$, the lowest-energy structure is no longer the cage structure (C_1), but the hybrid structure C_s. The hybrid structures based on stacked distorted cubic are also more stable than the other isomers. For $(MgO)_{12}$, the lowest-energy structure is not a cage structure (C_1), but the stacked ring C_{2h}. Then the stability of the clusters develops into a distorted cubic structure C_{2h} > the hybrid structures C_s based on hexagon ring and cubic > distorted cubic structure C_{2v}. For $(MgO)_{13}$, the stability of cage structure C_1 becomes the worst.

Table 2. The ΔG between MgO crystal and $(MgO)_n$ clusters at 700 K.

n	ΔG [kJ/mol]							
1	105.11							
2	52.65,	61.60						
3	32.31,	44.62						
4	13.63,	24.61,	22.45					
5	9.03,	20.20,	15.86,	16.69				
6	2.23,	2.17,	6.17,	6.41,	17.82			
7	-0.96,	1.20,	0.70,	0.09,	16.91			
8	-3.60,	-1.68,	-4.14,	16.01				
9	-6.89,	-5.48,	-6.66,	-2.37				
10	-6.83,	-6.54,	-7.37,	-7.90,	-6.02,	-6.56,	-4.54,	-7.33

11	-8.51,	-8.66,	-8.11,	-8.23		
12	-9.80,	-11.49,	-9.95,	-11.26,	-11.46,	-11.07
13	-12.16,	-9.13,	-11.81,	-11.72,	-11.56,	-11.48

In short, the $(MgO)_n$ clusters with linear or distorted cubic structures become more stable than the hexagon ring structures at 700 K, even the hybrid structures based on the hexagonal rings and distorted cubes are more stable than the cage structures. This explains that why the observed decomposition produces (MgO) of magnesite are cube nano-particles. Kim et al.[26] observed the structures of larger MgO clusters by using transmission electron microscopy and found that the cube-like nanoparticles with the edge length 2-3 nm.

Conclusions

The structure, stability and growth strategies of the $(MgO)_n$ (n = 1-13) clusters have been investigated by density functional theory. From reaction energy it can be seen that the contributions of the small clusters to grow is larger at lower temperature. By analyzing the differences in Gibbs free energy between MgO crystal and $(MgO)_n$ clusters, it can be seen that at the initial decomposition temperature of magnesite (about 700K), the $(MgO)_n$ clusters with linear or distorted cubic structures become more stable than the hexagon ring structures, even the hybrid structures based on the hexagonal rings and distorted cubes are more stable than the cage structures.

Acknowledgments

It was supported by the Project of Science and Technology of Anshan (Grant No.3983), and the National Natural Science Foundation of People's Republic of China (Grant No.11447110).

References

[1] M. -J. Malliavin, C. Coudray, *Ab initio* calculations on $(MgO)_n$, $(CaO)_n$, and $(NaCl)_n$ clusters (n=1–6), J. Chem. Phys. 106 **(**1997**)** 2323-2330.

[2] F. Bawa, I. Panas, Competing pathways for MgO, CaO, SrO, and BaO nanocluster growth, Phys. Chem. Chem. Phys. 4 (2002) 103-108.

[3] S.J.Clark, P.Jouanna, J.Haines, D.Mainprice, Calculation of infrared and Raman vibration modes of magnesite at high pressure by density-functional perturbation theory and comparison with experiments, Phys. Chem. Minerals. 38 (2011) 193-202.

[4] R. -N. Carlos, R. -A. Encarnacion, L. Ana, B. R -N. Alejandro, O. -H. Miguel, Thermal decomposition of calcite: Mechanisms of formation and textural evolution of CaO nanocrystals, Am. Mineral. 94 (2009) 578-593.

[5] D.-X. Fu, N.-X. Feng, Y.-W. Wang, Study on the Kinetics and Mechanism of Grain Growth during the Thermal Decomposition of Magnesite, Bull. Korean. Chem. Soc. 33 (2012) 2483-2488.

[6] C. Roberts, R. L. Johnston, Investigation of the structures of MgO clusters using a genetic algorithm, Phys. Chem. Chem. Phys. 3 (2001) 5024-5034.

[7] E. DelaPuente, A. Aguado, A. Ayuela, J. M. L´opez, Structural and electronic properties of small neutral $(MgO)_n$ clusters, Phys. Rev. B. 56 (1997) 7607-7614.

[8] L. Hong, H. Wang, J. Cheng, L. G. Tang, J. J. Zhao, Lowest-energy structures of $(MgO)_n$ (n = 2–7) clusters from a topological method and first-principles calculations, Comput. Theor. Chem. 980 (2012) 62-67.

[9] M. Haertelt, A. Fielicke, G. Meijer, K. Kwapien, M. Sierka, J. Sauer, Structure determination of neutral MgO clusters-hexagonal nanotubes and cages, Phys. Chem. Chem. Phys.14 (2012) 2849-2856.

[10] R. Dong, X. Chen, X. Wang, W. Lu, Structural transition of hexagonal tube to rocksalt for $(MgO)_{3n}$, $2 \leq n \leq 10$, J. Chem. phys. 129 (2008) 044705.

[11] K. Kwapień, Acitve Sites for Methane Activation in MgO and Li doped MgO, German, Humboldt-Universität zu Berlin, 2011,13-22.

[12] A. Jain, V. Kumar, M. Sluiter, Y. Kawazoe, First principles studies of magnesium oxide clusters by parallelized Tohoku University Mixed-Basis program TOMBO, Comp. Mater. Sci. 36 (2006) 171-175.

[13] B. Delley,An all-electron numerical method for solving the local density functional for polyatomic molecules, J. Chem. Phys. 92 (1990) 508-517.

[14] B. Delley, From molecules to solids with the $DMol^3$ approach, J. Chem. Phys. 113 (2000) 7756-7764.

[15] A.D. Becke, Density functional thermochemistry. III. The role of exact exchange, J. Chem. Phys. 98 (1993) 5648-5652.

[16] C. Lee, W. Yang, R.G. Parr, Development of the Colle-Salvetti correlation-energy formula into a functional of the electron density, Phys. Rev. B. 37 (1988) 785-789.

[17] J.M.Recio, R.Pandey, *Ab initio* study of neutral and ionized microclusters of MgO, Phys. Rev. A. 47 (1993) 2075-2082.

[18] J.M.Recio, A. Ayuela, R.Pandey, A.B.Kunz, Quantum mechanical calculations of stoichiometric MgO clusters, Z.Phys.D, 26 (1993) S237-S239.

[19] M.Haertelt, A.Fielicke,G. Meijer, K.Kwapien, M.Sierka, J.Sauer,Structure determination of neutral MgO clusters-hexagonal nanotubes and cages, Phys. Chem. Chem. Phys. 14 (2012) 2849-2856.

[20] P.J. Ziemann, A.W. Castleman Jr., Stabilities and structures of gas phase MgO clusters, J. Chem. Phys. 94 (1991) 718-728.

[21] Y. Zhang, H. S. Chen, Y H Yin and Y Song, Structures and bonding characters of $(MgO)_{3n}$ (n=2-8) Clusters, J. Phys. B: At. Mol. Opt. Phys. 47 (2014) 025102 (10pp)

[22] R. L.Stone, Thermal analysisi of magnesite at CO_2 pressures up to six atmospheres, J. Amceram. Soc. 37 (1954) 46-47.

[23] V. Jesenák , L.Turčániová , K.Tkáčová, Kinetic analysis of thermal decomposition of magnesite influence of generated defects and their annealing, Therm. Anal. 48 (1997) 93-106.

[24] B. V. L`vov, V. L.Ugolkov,Kinetics of free-surface decomposition of magnesium, strontium and barium carbonates analyzed thermogravimetrically by the third-law method, Thermochim. Acta. 409 (2004) 13-18.

[25] X.W.Liu,Y.L.Feng, H.R.Li, P.Zhang, P.Wang, Thermal decomposition kinetics of magnesite from thermogravimetric data, J. Therm. Anal. Calorim. 107 (2012) 407-412.

[26] M.G.Kim, U.Dahmen, A.W.Searcy, Structural transformations in the decomposition of $Mg(OH)_2$ and $MgCO_3$, J. Am. Ceram. Soc. 70 (1987) 146-154.